BIOCHEMISTRY
including biophysical chemistry & molecular biology
Article

Biochemistry **2010,** *49,* 2811–2820 2811
DOI: 10.1021/bi902087v

Sequence-Dependent Oligomerization of the Neu Transmembrane Domain Suggests Inhibition of "Conformational Switching" by an Oncogenic Mutant†

Andrew J. Beevers, Angeliki Damianoglou, Joanne Oates, Alison Rodger, and Ann M. Dixon*

Department of Chemistry, University of Warwick, Coventry CV4 7AL, U.K.

Received December 5, 2009; Revised Manuscript Received February 22, 2010

ABSTRACT: Membrane-spanning epidermal growth factor receptor ErbB2 is of key importance in cell division, in which a dimeric complex of the protein is responsible for tyrosine kinase activation following ligand binding. The rat homologue of this receptor (Neu) is prone to a valine to glutamic acid mutation in the transmembrane domain (TM), resulting in permanent activation and oncogenesis. In this study, the TM domains of Neu and the corresponding oncogenic mutant Neu*, which contains a V to E mutation at position 664 in the TM domain, have been analyzed to improve our understanding of the structural effects of the oncogenic $V_{664}E$ mutation. Building on previous work, we have focused here on understanding the sequence dependence of TM helix−helix interactions and any differences in behavior upon introduction of the $V_{664}E$ mutation. Using a variety of biochemical and biophysical methods, we find that the rat Neu TM domain forms strong oligomers and, similar to previous observations for the human ErbB2 TM domain, the oncogenic mutation results in a reduced level of self-association. Our data also strongly indicate that the proto-oncogenic Neu TM domain can adopt multiple (at least two) oligomeric conformations in the membrane, possibly corresponding to the active and inactive forms of the receptor, and can "switch" between the two. Further, the oncogenic Neu* mutant appears to inhibit this "conformational switching" of TM dimers, as we observe that dimerization of the Neu* TM domain in the *Escherichia coli* inner membrane strongly favors a single conformation stabilized by an I*XXX*V motif (I_{659}-*XXX*-V_{663}) originally identified by site-specific infrared spectroscopic studies.

ErbB2 is a member of the epidermal growth factor (ErbB) family of receptor tyrosine kinases (RTKs)[1] and contains an extracellular ligand binding domain, an α-helical transmembrane (TM) domain, and an intracellular tyrosine kinase domain. The ErbB2 receptor is activated by ligand-dependent dimer formation, triggering activation of the tyrosine kinase and promoting cell division (*1*−*3*). The rat form of the ErbB2 receptor (termed the Neu proto-oncogene) is susceptible to a mutation in its TM domain that causes permanent activation of the tyrosine kinase, resulting in oncogenic activity (*4*−*7*). This mutant (here termed Neu*) contains a glutamic acid residue in place of Val_{664} in the TM domain [$V_{664}E$ (Figure 1A)], and this mutation results in the development of cancer. A similar mutation ($V_{659}E$) in the human ErbB2 protein also causes constitutive receptor activation (*8*). Therefore, investigation of the structural consequences of the Neu* mutation is critical to our understanding of the underlying mechanism of oncogenesis in this protein and potentially a range of other RTKs that are highly important in both human and animal health.

To improve our understanding of the oncogenic effects of the $V_{664}E$ mutation, the TM domains of the Neu and Neu* proteins have been studied extensively in the past. The secondary structures of both proteins have been shown to be largely α-helical; however, there is still disagreement about whether the mutation leads to a reduction or increase in helicity (*9*−*13*) or whether the mutation causes a decrease in the level of kinking of the wild-type helix (*14*). Likewise, the oligomeric states of the two TM domains have also been studied (*10*, *12*, *13*, *15*) with a similar lack of consensus with regard to the effects of the mutation. Depending on the technique used for measurement, some studies have reported that both TM domains dimerize to similar degrees (*10*, *12*, *15*), others report that wild-type Neu is more dimeric than the Neu* mutant (*13*), while still other studies suggest the opposite is true (*6*, *16*). Furthermore, studies on the closely related human ErbB2 protein suggest that the TM domain forms weak trimers (*17*). This variation in results is most likely due to the fact that the solution conditions required by the wide variety of applied techniques may lead to relative stabilization or destabilization of TM helix oligomers.

High-resolution techniques such as nuclear magnetic resonance and site-specific isotopically labeled infrared spectroscopy have also been used to propose various structural models for the Neu* TM domain dimer to help explain the structural impact of the point mutation (*9*, *18*, *19*). Initially, it was reported that direct hydrogen bonding between E_{664} residues on separate Neu* monomers, which studies have shown are protonated, promoted permanent dimerization of the TM domain (*18*). However, this

†This work was supported by the Medical Research Council (Grant G0601114).

*To whom correspondence should be addressed. Telephone: 0 (44) 24761 50037. Fax: 0 (44) 24765 24112. E-mail: ann.dixon@warwick.ac.uk.

[1]Abbreviations: ATR-FTIR, attenuated total internal reflection Fourier transform infrared; CAT, chloramphenicol acetyltransferase; CD, circular dichroism; DMPC, dimyristoylphosphocholine; DMPS, dimyristoylphosphoserine; DOF, degrees of freedom; DPC, dodecylphosphocholine; EGF, epidermal growth factor receptor; ESI-TOF-MS, electrospray ionization time-of-flight mass spectrometry; GpA, glycophorin A; HPLC, high-performance liquid chromatography; LD, linear dichroism; LUV, large unilamellar vesicle; MBP, maltose binding protein; RTK, receptor tyrosine kinase; SDS−PAGE, sodium dodecyl sulfate−polyacrylamide gel electrophoresis; TFA, trifluoroacetic acid; TFE, trifluoroethanol; TM, transmembrane.

Published on Web 02/24/2010

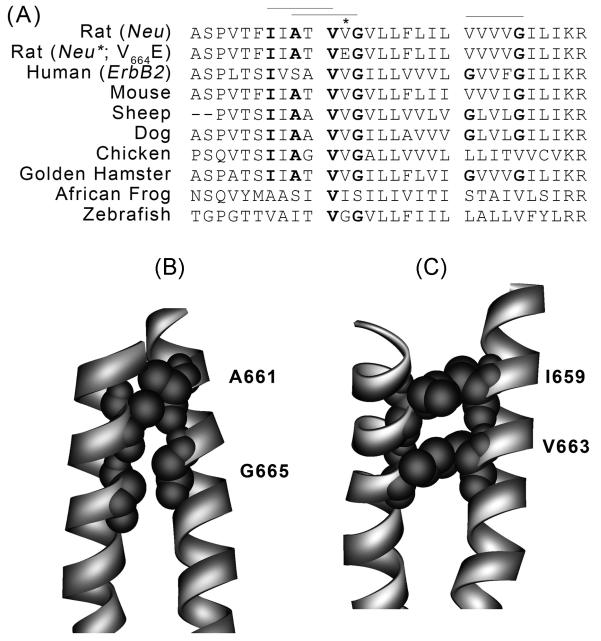

FIGURE 1: Transmembrane domain sequences and motifs of rat Neu and closely related mammalian homologues. (A) Sequence alignment of the Neu, Neu*, and ErbB2 TM domains from various organisms. Note the consistent occurrence of the I*XXX*V motif in a majority of the sequences. The A*XXX*G motif is conserved across many species; in humans, however, it exists as the structurally similar S*XXX*G motif. Also note the lack of a G*XXX*G motif in the C-terminal region of the rat TM domain, while this motif is present in the human form. (B) Molecular model illustrating the interface of the Neu* TM domain dimer proposed by solid-state NMR (*9*), consisting in part of residues A_{661} and G_{665} forming an A*XXX*G motif. (C) Molecular model showing the interface of the Neu* TM domain dimer proposed by site-specific infrared dichroism studies (*19*), consisting of a motif including residues I_{659} and V_{663} (I*XXX*V motif).

interaction has not been observed in any computational investigations (*20*, *21*) or subsequent spectroscopic studies (*9*, *19*) performed on the TM domain. Other proposed models include hydrogen bonding of E_{664} to carbonyl groups in the α-helical backbone of the protein (*22*) as well as interaction of water molecules with the E_{664} residue, although the role of these water molecules in dimer formation is unknown (*19*, *23*−*26*). Apart from direct participation of E_{664} in helix−helix interactions, two additional sequence motifs have been highlighted as potentially packing at the interface of the helical Neu* TM domain dimer: a motif consisting of A_{661} and G_{665} residues (*9*) [known as the Sternberg−Gullick motif (*27*) (Figure 1B)], similar to the standard G*XXX*G motif seen in many transmembrane α-helical oligomers (*28*), and a motif consisting in part of I_{659} and V_{663} residues (Figure 1C) (*19*). Both motifs are highly conserved across many species (Figure 1A), and site-directed mutagenesis of the TM domain in the full-length protein has indicated that residues close to position 664 (in particular A_{661}, V_{663}, and G_{665}) may be very important to the activation of the protein (*29*).

However, with regard to how the V_{664}E mutation in Neu* affects structure and dimer formation, there are currently no high-resolution experimental data for the wild-type Neu protein for comparison. The best approximation thus far is the recently reported high-resolution NMR structure of the human ErbB2 TM domain dimer (*30*), which shows an N-terminal S*XXX*G motif at the dimer interface, similar to the A*XXX*G motif suggested by solid-state NMR for the Neu* dimer (*9*). This structure for human ErbB2 is considered to be the active-state dimer, associating via the N-terminal G*XXX*G-like motif; however, the human ErbB2 TM domain also contains a C-terminal G*XXX*G motif that is thought to stabilize the inactive-state dimer (*31*). A very recent study has shown that the S*XXX*G motif has a slightly higher propensity to self-associate than the G*XXX*G motif, further suggesting that this motif may be more critical for receptor dimerization (*32*). From this and other studies of ErbB2, Neu, and other RTKs, a model of "conformational switching" between the active and inactive states has emerged. In this model, elegantly demonstrated for the EGF receptor (*33*), dimerization is not itself the cause of RTK activation, as several RTKs have been shown to exist as preformed dimers. Instead, it was suggested that some conformational change (e.g., rotation) upon binding of ligand caused activation of the receptor (*34*). This same "flexible rotation" or "molecular switch" model has been proposed for Neu* (*18*), and although it has not yet been confirmed experimentally, it is further strengthened by computational mapping studies of the human ErbB2 TM domain, indicating two local energy minima corresponding to the proposed active and inactive dimers. Fleishman and co-workers showed that the potential energy barrier between these two minima is relatively low, therefore permitting "switching" between the two states by small structural or energetic changes to the TM domain that are likely to by caused by ligand binding or mutation (*31*).

Building on this previous work, we sought here to explore the sequence dependence of TM helix−helix interactions in the wild-type Neu TM domain homodimer and any differences in behavior upon introduction of the V_{664}E oncogenic mutation (i.e., Neu*). The propensity of wild-type rat Neu and Neu* TM domains to self-associate in the inner membrane of *Escherichia coli* has been studied for the first time using the TOXCAT assay, and we show that, while both interact strongly, the V_{664}E mutation results in a significant decrease in the level of self-association. We have also investigated the roles of the A_{661}-*XXX*-G_{665} and I_{659}-*XXX*-V_{663} motifs in TM helix interactions; they reveal clear and striking differences in the behavior of the wild-type and oncogenic proteins. Our data strongly support a single, previously reported model for the mutant Neu* TM domain dimer containing I_{659} and V_{663} at the dimer interface. Comparison of data for the equivalent mutations in the wild-type Neu TM domain indicated that this domain can adopt multiple oligomeric conformations in the membrane. Taken together, our data suggest that the V_{664}E mutation does not cause oligomerization of monomeric Neu but instead causes a change in the preferred conformation of the dimer and potentially prevents conformational switching to the inactive state.

EXPERIMENTAL PROCEDURES

TOXCAT Assay. The self-association of the wild-type rat Neu TM domain, as well as the Neu* TM domain and several mutants, was studied using the TOXCAT assay (*35*). Briefly, TOXCAT employs a chimeric protein in which the α-helical TM domain of interest is inserted between the N-terminal DNA binding domain of ToxR, a dimerization-dependent transcriptional activator, and maltose binding protein (MBP), a monomeric periplasmic anchor protein. The fusion protein is constitutively expressed in *E. coli* together with a chloramphenicol acetyltransferase (CAT) reporter gene under the control of a ToxR-responsive ctx promoter. Oligomerization of the TM domains within the bacterial inner membrane results in oligomerization of the ToxR

domain, transcriptional activation of the ctx promoter, and CAT expression. The amount of CAT expressed in this system is proportional to the strength of oligomerization of the TM domains. The expression vectors (pccKAN, pccGpA-wt, and pccGpA-G_{83}I) and *E. coli* strain NT326 were kindly provided by D. M. Engelman (Yale University, New Haven, CT). TOXCAT chimera containing the TM domains of interest were constructed according to a reported protocol (*35*) and expressed in *E. coli*. Expression levels for all constructs were confirmed via Western blot analysis using antibodies against the MBP domain prior to the performance of CAT assays. Correct insertion and orientation of all chimeras in the *E. coli* inner membrane were confirmed using the *malE* complementation assay (*35*) in which cells were grown on M9 agar plates containing 0.4% maltose. CAT assays were performed using the FAST CAT Green (deoxy) Chloramphenicol Acetyltransferase assay kit (Molecular Probes, Invitrogen) according to the manufacturer's instructions.

The resulting CAT activities were normalized for total fusion protein expression using ImageJ to quantitatively analyze expression levels (i.e., intensities of bands) in anti-MPB Western blots of each chimera. Statistical evaluation of all TOXCAT data for wild-type (wt) Neu and Neu* and the various mutants was then conducted using a Student's *t* test with four degrees of freedom (DOF = 4) and a probability (*p*) of 0.05 (95% confidence interval) to establish whether the effect of a given mutation was significant within error.

Peptide Synthesis and Purification. Synthetic peptides corresponding to the TM domain of the wild-type rat Neu protein (residues 652−684, RASPVTFIIATVVGVLLFLILVVVVGILIK RRR, molecular mass of 3630 Da) and the oncogenic mutant Neu* (residues 652−684, RASPVTFIIATVEGVLLFLILVVVVGILIKRRR, molecular mass of 3663 Da) were synthesized using solid-phase F-moc methods at the W.M. Keck Facility at Yale University. The peptides were purified by reversed-phase HPLC using a linear acetonitrile gradient including 0.1% trifluoroacetic acid (TFA) on a C4 Jupiter column (Phenomenex). The purity of pooled peptide fractions was confirmed by electrospray ionization time-of-flight mass spectroscopy (ESI-TOF-MS microTOF, Bruker) before subsequent lyophilization. Peptides were stored as dry powders until they were used.

Circular Dichroism (*CD*). CD spectra of the Neu and Neu* TM peptides were recorded in 2,2,2-trifluoroethanol (TFE), detergent micelles, and a synthetic lipid bilayer. All samples were prepared at a peptide concentration of ~0.2 mg/mL. The detergent samples were prepared via addition of the peptide to a solution of 15 mM dodecylphosphocholine (DPC) (Avanti Polar Lipids, Alabaster, AL) detergent, 50 mM sodium phosphate buffer (NaP_i, pH 7.3), and 150 mM NaCl. We prepared large unilamellar vesicles (LUVs) containing either the Neu or Neu* TM peptide by codissolving 1,2-dimyristoyl-*sn*-glycero-3-phosphocholine [DMPC, which has been used in previous studies of this TM domain (*18*, *19*)] and an aliquot of peptide dissolved in TFE. The TFE was removed under a nitrogen flow and placed under vacuum overnight to remove residual organic solvent. The lipid film was then resuspended in 10 mM Bis Tris Propane (pH 7), using a vortex mixer and a sonication bath held at 31 °C. The vesicles were subjected to five freeze−thaw cycles using a bath of dry ice and ethanol, followed by slow thawing at room temperature. To form homogeneous LUVs, the sample was then extruded through a 100 nm polycarbonate membrane. CD spectra were recorded using a Jasco J-815 spectropolarimeter (Jasco UK, Great Dunmow, U.K.) and 0.2 mm path length quartz cuvettes (Starna, Optiglass Ltd., Hainault, U.K.). Spectra were recorded between 190 and 260 nm with a data pitch of 0.2 nm, a bandwidth of 2 nm, and a scanning speed of 100 nm/min. Data shown were averaged from 16 individual spectra and were truncated at 190 nm, below which the absorbance was too high to give reliable data. Measurement of TFE, DPC micelles, or DMPC vesicles without peptide was subtracted to yield the final spectra. The CD data are plotted in units of (mol of amino acid residues)$^{-1}$ dm^3 cm^{-1}. The α-helical content of the peptides was estimated by assuming that 100% helicity corresponded to -12 mol^{-1} dm^3 cm^{-1} at 208 nm (*36*, *37*).

Linear Dichroism (*LD*). DMPC vesicles containing either the Neu or Neu* TM peptide were prepared as described for the CD measurements. The resulting samples were placed into a capillary in a microvolume LD cell (Crystal Precision Optics Rugby, now available from Kromatek, UK). A stationary quartz rod was inserted into the capillary, and the capillary was then rotated. The annular gap that contains the sample was 250 μm, making a total path length of 500 μm. Data were collected on a Jasco J-815 spectropolarimeter. The data were measured at 0.2 nm intervals from 190 to 260 nm. The spectra were recorded at room temperature with the Couette cell rotating at 3 V (approximately 3000 rpm). A spectrum of the nonrotating sample was subtracted to yield the final spectrum in each case. A light scattering correction of the form $a\lambda^{-k}$ was applied, where λ is the wavelength and a and k are constants. In this case, $k = -4.1$ for Neu and $k = -2.8$ for Neu*.

RESULTS AND DISCUSSION

TM Domains of Rat Neu and the Oncogenic $V_{664}E$ Mutant, Neu, Strongly Self-Associate in Natural Membranes, but Neu* Associates More Weakly*. It has been shown in the past that the TM domain of the ErbB2 protein, the human homologue of the rat Neu proto-oncogene, self-associates in vivo (*32*, *38*). Specifically, the TOXCAT assay, a ToxR-based transcriptional assay linked to chloramphenicol acetyltransferase (CAT) expression (*35*), was used to measure the propensity of the ErbB2 TM domains to homo-oligomerize in the inner membrane of *E. coli*. The strength of this interaction was classified as strong and was thought to occur via interaction of one or more G*XXX*G motifs in the TM domain sequence (*32*, *38*). In our study, we have made the complementary measurements for the TM domains of wild-type Neu and its oncogenic $V_{664}E$ mutant (Neu*) to compare their self-association behavior in the *E. coli* inner membrane.

The sequences corresponding to the respective TM domains of rat Neu and the oncogenic Neu* investigated using the TOXCAT assay are shown in Figure 2, along with the resulting CAT activities. In the TOXCAT assay, the degree of TM helix−helix self-association is proportional to the CAT activity (see Experimental Procedures). Western blots are shown below the TOXCAT data to confirm the expression of each of the protein chimeras, and the results presented in Figure 2 have been normalized for expression level (see Experimental Procedures). The correct insertion and orientation of the chimeric proteins into the *E. coli* inner membrane were confirmed using the *malE* complementation assay (see Experimental Procedures). It should be mentioned that the *malE* complementation assay does confirm membrane insertion but cannot distinguish the actual fraction of chimeric protein reaching the membrane. Because the Neu* sequence carries a Val to Glu mutation, one might expect that

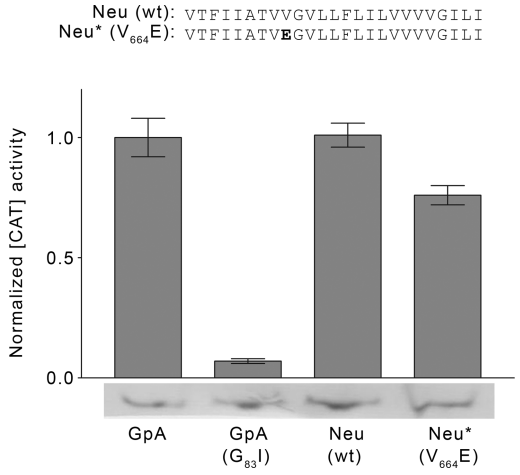

FIGURE 2: Oligomerization of transmembrane domain sequences of rat Neu and Neu* in *E. coli* membranes. Rat Neu and Neu* TM domain sequences analyzed using the TOXCAT assay. Below the sequences, the CAT activities obtained in the TOXCAT assay are shown for the wild-type Neu and the oncogenic Neu* mutant and for positive [glycophorin A TM (GpA)] and negative (GpA G_{83}I mutant) controls. CAT activities are means (after normalization to fusion protein concentration, and then to the value for GpA) of three or more independent measurements ± the standard error of the mean (SE). Western blots against maltose binding protein (MBP) are shown below the TOXCAT data to confirm expression levels of each fusion protein.

this would exert a significant insertion penalty near the center of the sequence. Nonetheless, calculation of the apparent free energy of insertion (ΔG_{app}) using the scale of Hessa and von Heijne (*39*) indicates that each of the sequences analyzed using the TOXCAT assay would be predicted to insert into the cytoplasmic membrane (i.e., favorable ΔG_{app}).

TOXCAT data were also obtained for a positive control, namely, the fully structurally elucidated TM domain of glycophorin A (GpA) (*40*) which is known to dimerize strongly (*41*), and for a negative control, a point mutant of GpA, G_{83}I, which greatly reduces the population of dimers. Comparison of the results using a Student's *t* test (DOF = 4; $p = 0.05$; see Experimental Procedures) indicated that there was no significant difference between the signals from the wild-type Neu TM domain and that of GpA, demonstrating the intrinsic ability of the wt Neu TM domain to self-associate in a natural membrane environment.

Comparison of these data with the previous TOXCAT data for the human ErbB2 TM domain, which yielded CAT activities at approximately 50% of GpA levels, suggests that the self-association of the rat Neu TM domain is stronger than that observed for its human homologue. The fact that the magnitude of the signal for the Neu TM is higher than that for ErbB2 is somewhat surprising, but similar strong oligomerization has been observed in the past when using the TOXCAT assay to analyze several other TM domains (*42*, *43*). The enhanced CAT activity observed here for Neu may be due to differences in the lengths of the rat Neu TM domains analyzed in this study (25 residues) and the TM domain of the human ErbB2 protein studied by Mendrola et al. (22 residues) (*38*). However, it has previously been noted [Z. Jenei, unpublished results, and Li et al. (*44*)] that a decrease in CAT activity (not the increase observed in this study) results when the length of the TM domain inserted into the TOXCAT chimera is systematically increased, presumably due to a forced change in the tilt angle of the TM domain caused by the limited hydrophobic area of the membrane. Therefore, although our results were reproducible, rather than quantitatively compare them with literature data, in this work we simply used this assay to measure the relative effect of mutations within each TM domain.

The behavior of Neu directly reflects that of its human homologue with respect to the effect of the oncogenic mutation on TM self-association. Comparison of the data obtained for the wt Neu TM domain and the Neu* mutant (Figure 2, V_{664}E) using a Student's *t* test (DOF = 4; $p = 0.05$) indicates that the V_{664}E mutation in the Neu* TM domain results in a moderate but significant decrease in the level of homo-oligomer formation to approximately 75% of wild-type levels. This same effect was observed for the ErbB2 TM domain (*38*) upon introduction of the homologous V_{659}E mutation, suggesting that residues in this position play a role in stabilizing the TM oligomer.

It is worth noting that this difference in homo-oligomerization was not observed in SDS when we analyzed peptides corresponding to the TM domains of rat Neu and Neu* (residues R_{652}–R_{684}) using SDS–PAGE (see Figure S1 of the Supporting Information), an experiment that was conducted because the TOXCAT assay cannot report on the oligomeric state. Using SDS–PAGE, both peptides migrated as single bands at ~6 kDa. This mass is very near that of the peptide dimer (7.2 kDa), in keeping with previous reports that the Neu TM domain is dimeric (*10*, *13*, *17*), and suggests that our Neu and Neu* TM peptides both form very stable dimers in SDS. However, the potential for antiparallel (non-native) dimer formation in micelles, an orientation not likely to occur in the TOXCAT chimera, cannot be excluded here and could explain the conflicting TOXCAT and SDS–PAGE results. Furthermore, a recent report gives details of anomalous migration of transmembrane proteins due to detergent binding during SDS–PAGE analyses (*45*), with the result that monomeric peptides bind sufficient SDS to make them migrate as higher-molecular mass species (e.g., mistaken for dimers). This cannot be ruled out here and is in agreement with previous reports that the Neu and Neu* TM domain peptides migrate primarily as monomers or as a mixture of monomers and dimers on SDS–PAGE (*12*, *13*). If it is the case that SDS is denaturing the peptide dimers, and the band at 6 kDa is actually a monomer with a significant amount of bound SDS, this may explain why both peptides behave identically using SDS–PAGE despite the clear differences observed for the two sequences in the less denaturing environment of a natural membrane bilayer (i.e., in the TOXCAT assay).

Both Neu and Neu TM Peptides Spontaneously Insert across Lipid Bilayers, and No Differences Are Observed in Their Secondary Structures*. With clear differences between the Neu and Neu* TM domains being observed in a natural membrane bilayer using the TOXCAT assay, but with no difference in the oligomeric state being observed using SDS–PAGE, we sought to investigate whether differences in the interactions of Neu and Neu* TM domains with membrane bilayers (i.e., their ability to insert as α-helices into bilayers) could explain their different behavior in vivo. The insertion of the TM domains of Neu and Neu* into lipid bilayers has not been thoroughly investigated in the literature, which is surprising considering the large number of studies of human ErbB2 and rat Neu TM domains in vesicles and liposomes. Thus far, only the calculated α-helical orientation from polarized ATR-FTIR has

been used as a measure of insertion of the TM domain into DMPC (*19*) and DMPC/DMPS bilayers (*18*). A key limitation of FTIR is the use of stacked partially hydrated multilayers as opposed to fully hydrated spherical vesicles in solution, which is more representative of an actual cell membrane. The low degree of hydration may affect the secondary structure of the peptide and possibly induce a greater propensity for nonspecific peptide aggregation. Therefore, to avoid some of these issues and study the insertion of Neu and Neu* TM domains in solution in a fully hydrated bilayer, thus producing more biologically relevant and potentially new information, we report here the use of flow linear dichroism (LD) spectroscopy (*46*, *47*) to investigate the insertion of peptides corresponding to the TM domains of rat Neu and Neu* (see Experimental Procedures).

Recent technical advances in LD have enabled the routine use of small sample volumes (< 50 μL) (*48*, *49*), facilitating its application to the study of membrane proteins (*46*, *50*). The signal obtained in LD results from the difference in absorption of horizontally and vertically polarized light by a sample aligned parallel to one of the polarization axes (usually the horizontal direction). Therefore, samples for flow LD must be capable of being aligned in shear flow, which means that the molecules under investigation must be asymmetric in shape. Liposomes are well-suited to this technique as they are distorted in shear flow and can be flow-aligned in a rapidly spinning Couette cell to produce elongated shapes. If there is no interaction between the peptide and liposomes, the peptide will not align, and therefore, no difference in the absorption of the two polarizations of light (LD signal) will be observed. If the peptide inserts as an α-helix across the bilayer (i.e., orients perpendicular to the plane of the membrane), broad positive LD signals centered at approximately 195 and 220 nm will be observed. These signals are due to the $\pi \rightarrow \pi^*$ and $n \rightarrow \pi^*$ transitions of the peptide bond (see Figure 3A for a schematic), respectively, which are polarized perpendicular to the helical axis. A broad negative (or in practice less positive) signal may also be observed at ~208 nm, corresponding to the $\pi \rightarrow \pi^*$ transition of the peptide bond polarized parallel to the helical axis; however, the 208 nm signal is often masked by the two positive signals on either side of it. For peptides lying on the surface of the membrane (i.e., oriented parallel to the plane of the bilayer), the signals will be opposite in sign with, e.g., a negative LD signal at 195 nm.

The Neu and Neu* TM domain peptides were studied in flow-aligned 1,2-dimyristoyl-*sn*-glycero-3-phosphocholine (DMPC) vesicles using LD, and the resulting spectra are shown in panels B and C of Figure 3 for Neu and Neu*, respectively. DMPC was selected as a membrane mimetic because the majority of previous work on the Neu TM domain has been performed in DMPC vesicles (*18*, *19*), thus offering a good base for comparison. We consider first the simpler Neu* LD spectrum (Figure 3C), which shows a positive peak at 190 nm and a negative peak at 208 nm [this is particularly clear in the light scattering-corrected spectrum (dashed line in Figure 3C)]. Surprisingly, there is no evidence of the $n \rightarrow \pi^*$ band at 222 nm. Usually, the 208 nm band is observed as a minimum between two maxima of the same sign at 222 and 195 nm. The absence of a large signal at 222 nm means that the 208 nm band is actually observed as a negative signal. This is the first time we have seen the 208 nm band as a clear independent signal in a spectrum. To understand these relative magnitudes, we need to consider the equation that describes the LD signal in a liposome system. The relative magnitudes of LD bands are

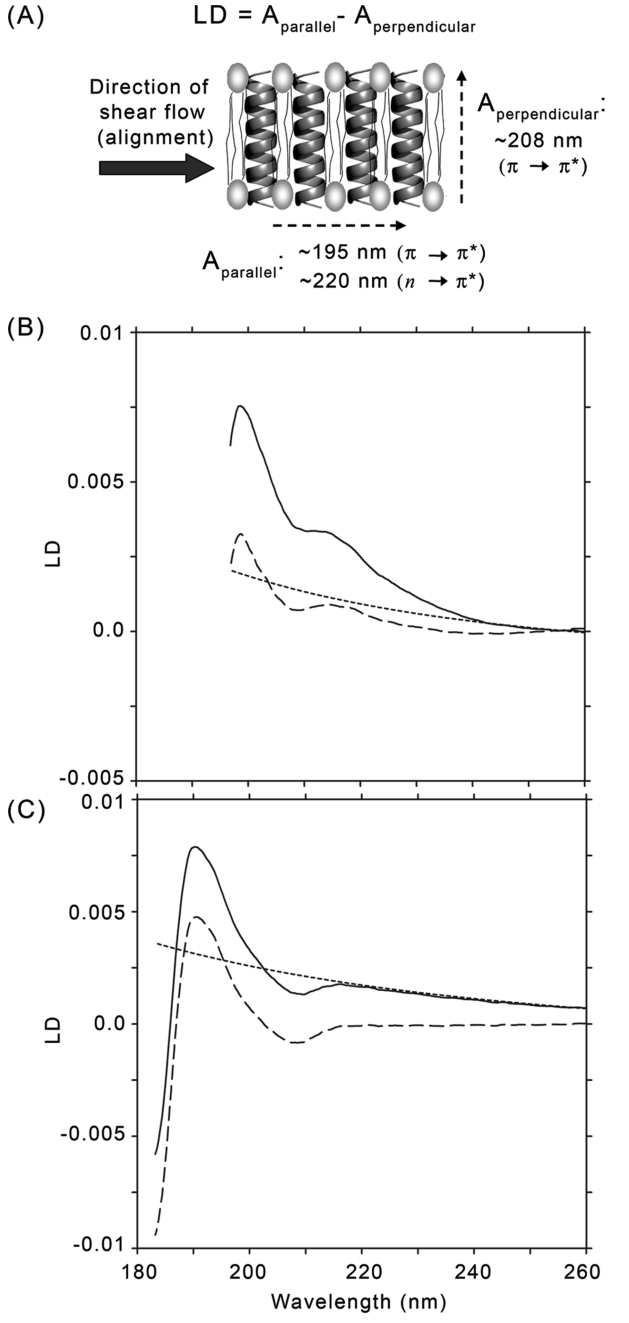

FIGURE 3: Study of membrane insertion using linear dichroism (LD) spectroscopy. (A) LD of the Neu and Neu* peptides in lipid vesicles depends on the alignment of vesicles by shear flow. The direction of the flow is indicated by an arrow and is considered the "parallel" direction (where LD = $A_{parallel} - A_{perpendicular}$). Peptides associated with lipid bilayers, such as Neu and Neu*, yield a signal in LD that depends on their orientation in the bilayer. As shown in the schematic, the $n \rightarrow \pi^*$ transition of the peptide bond in a transmembrane α-helix is aligned parallel to the direction of flow and thus yields a positive LD signal at ~220 nm. Conversely, the $\pi \rightarrow \pi^*$ transition is aligned perpendicular to the direction of flow and thus yields a negative LD signal at ~208 nm. Comparison of LD spectra of (B) wild-type Neu and (C) mutated Neu* in DMPC vesicles at a peptide concentration of 0.27 mg/mL and a lipid concentration of 2.7 mg/mL. In panels B and C, the LD spectra are shown before (—) and after (– – –) the subtraction of a light scattering correction (· · ·) (see Experimental Procedures for more details). The LD data were acquired using a cell with a path length of 0.5 mm rotating at 3 V. The positive peak at ~195 nm, the negative peak at 208 nm, and the positive peak at ~217 nm observed in both LD spectra are indicative of a helical peptide inserted across the bilayer in a transmembrane orientation (*46*).

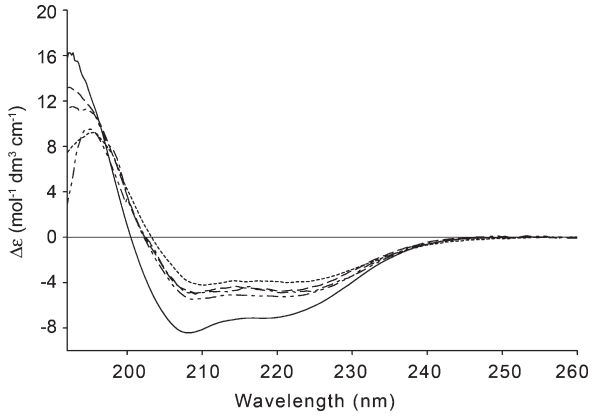

FIGURE 4: Secondary structure of Neu and Neu* TM domains. CD spectra of Neu and Neu* in TFE (—), Neu in DPC (· · —· ·) and DMPC (· · ·), and Neu* in DPC (— — —) and DMPC (· —·). CD data are expressed in units of $\Delta\varepsilon$ (mol^{-1} dm^3 cm^{-1}), using the concentration of amino acids in the calculation to normalize any effects of small differences in concentration, and were obtained using a cuvette with a path length of 0.2 mm. The negative peaks at 208 and 220 nm are indicative of significant α-helical secondary structure.

determined by the relative magnitudes of their absorbance and their angle factors (*46*, *51*):

$$\frac{3}{4}(1 - 3\cos^2\beta)$$

where β is the tilt angle of the peptide in the membrane. At a tilt of 0° with respect to the membrane normal, the 222 nm:210 nm ratio is −0.5; at 30°, it is −0.2, and at 36°, it is 0.04. Thus, LD suggests that Neu* is tilted at more than 30° from the membrane normal. (Work is in progress to make such estimates more quantitative, but it requires an accurate value for the absorption intensities of the two bands.) At first sight, the wt Neu TM LD spectrum (Figure 3B) looks quite different from that of Neu*. However, closer inspection shows the same features, with a positive peak below 200 nm and a small negative peak at 208 nm. (The data were harder to collect due to increased light scattering in the sample, thus limiting the reliable wavelength range.) The negative peak at 208 nm again tells us that the peptide is tilted. However, the presence of positive intensity at 220 nm indicates the tilt angle of Neu in the membrane is smaller than that for Neu*.

The LD data thus provide strong evidence that both the Neu and Neu* TM peptides spontaneously insert as transmembrane α-helices into fully hydrated (i.e., solution-phase) DMPC bilayers, but that the tilt of the Neu* TM domain is slightly larger than that of Neu. Our ATR-FTIR data support these conclusions as shown in Figure S2 of the Supporting Information; these results also agree well with previous studies of Neu* in DMPC (*18*, *19*).

Solution-state circular dichroism (CD) spectra were recorded for each peptide reconstituted in DMPC vesicles, as well as TFE and DPC detergent micelles for the sake of comparison (see Figure 4), and all spectra exhibited a characteristic α-helical profile with negative maxima at 208 and 222 nm, demonstrating that both peptides are significantly α-helical under all conditions studied. Interestingly, very little difference is observed between the CD spectra of wild-type and mutant Neu in any of the solution conditions studied. As one can see in Figure 4, the spectra for the two peptides in each solvent either completely overlay one another (TFE) or are very close in intensity and shape. These data are in agreement with previous studies that report similar levels of helicity in the two proteins (*12*, *13*, *18*, *52*) and indicate that secondary structure changes are also not the source of the differences observed between Neu and Neu* in both TOXCAT and in vivo.

Neu and Neu TM Domain Oligomers Are Stabilized by Different Helix−Helix Interaction Motifs*. Having observed no significant differences between the secondary structure or membrane interactions of the Neu and Neu* TM peptides in DMPC bilayers in vitro, and no differences in oligomeric state by SDS−PAGE, we explored the possibility that the conformations of the two TM domain dimers are in some way fundamentally different and that these differences are sequence-dependent. Indeed, this hypothesis that the $V_{664}E$ mutation changes the relative orientation of the two TM helices relative to one another has been suggested by several groups (*18*, *31*, *38*). As mentioned above, two sequence motifs have been specifically highlighted in the literature as potentially packing at the interface of the oncogenic Neu* TM domain dimer: an A*XXX*G motif consisting of A_{661} and G_{665} residues (*9*, *27*) (Figure 1B), similar to the S*XXX*G motif found at the dimer interface of the human ErbB2 TM domain dimer (*30*), and a motif consisting in part of I_{659} and V_{663} residues [I*XXX*V (Figure 1C)] (*19*). To determine whether either motif was participating in key helix−helix interactions of Neu and Neu* TM domain dimers in natural membrane bilayers, we again used the TOXCAT assay. Single, double, or quadruple mutations of the wild-type sequences previously analyzed using the TOXCAT assay (Figure 2) were prepared, and the resulting effect on CAT activity was measured.

Panels A and B of Figure 5 show the sequences of the various Neu and Neu* TM domain mutants studied and the corresponding CAT activities observed, as well as the Western blots used to normalize data to protein concentration. In Figure 5A, the results are given for the wild-type Neu TM domain and two double mutants [data normalized to GpA (shown in Figure 2)] designed to disrupt packing of the I*XXX*V motif ($I_{659}A/V_{663}L$) or the A*XXX*G motif ($A_{661}L/G_{665}L$). Comparison of the data obtained for the wt Neu TM domain with these two double mutants using a Student's *t* test (DOF = 4; $p = 0.05$) indicates that both mutants have similar and moderate but significant effects on the measured CAT activity, each one reducing it by ~25% compared to that of wild-type Neu. Also of interest is the fact that both of these double mutants yield the identical reduction in CAT activity observed for the Neu* oncogenic mutation ($V_{664}E$), which also yielded an ~25% reduction in CAT activity compared to wild-type levels (Figure 2).

The levels of CAT expression measured for the double mutants indicate that, while mutation of each motif does moderately destabilize Neu TM oligomers (or initiate a conformational rearrangement), each of the double mutants still retains the ability to form relatively strong oligomers. This suggests that both motifs shown in panels B and C of Figure 1 are of equal importance. In support of this, when both of these motifs are mutated simultaneously to produce the quadruple $I_{659}A/A_{661}L/V_{663}L/G_{665}L$ mutant, there is even further reduction in CAT activity to approximately 47% of wild-type CAT levels (Figure 5A), a much more significant effect (as confirmed by a *t* test; DOF = 4; $p = 0.05$). Taken together, these results suggest that both the I*XXX*V and A*XXX*G motifs are viable sites of helix−helix interactions and that they likely represent the highest-affinity interaction sites in the Neu TM domain dimer. It is interesting to note that while we have managed to reduce the affinity by 53% by mutating both motifs, the levels of CAT

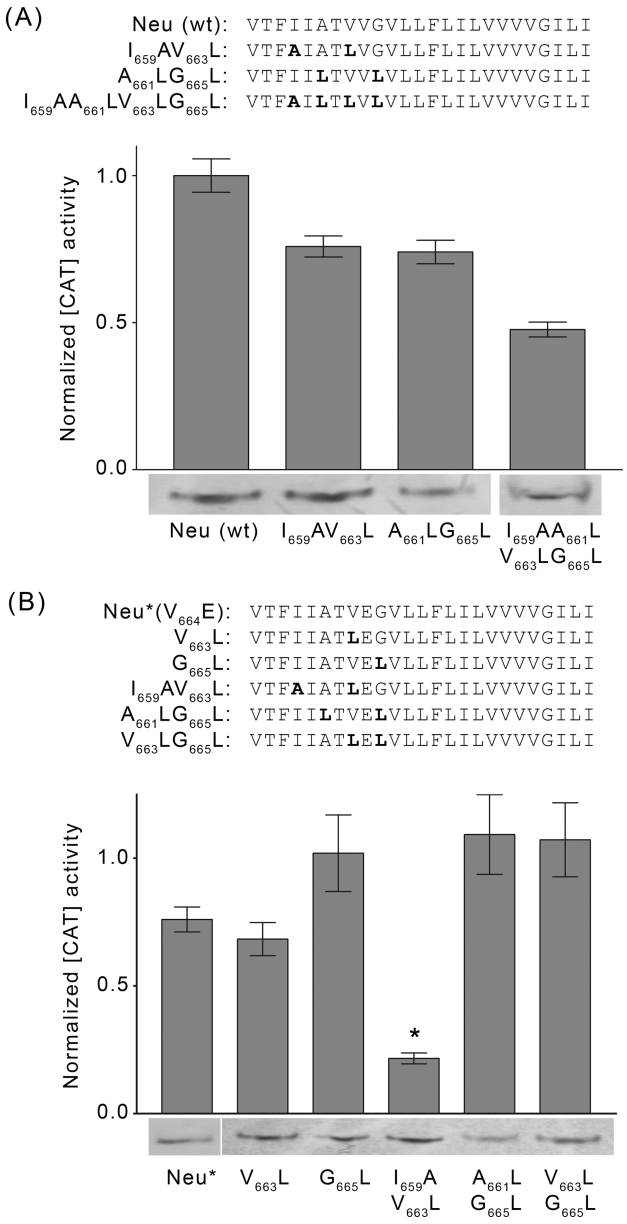

FIGURE 5: Oligomerization of rat Neu and Neu* transmembrane domain mutants in *E. coli* membranes. (A) Wild-type Neu TM domain sequence and those of three mutants, designed to knock out key A*XXX*G and I*XXX*V motifs from literature (*9*, *19*), and the resulting CAT activities obtained in the TOXCAT assay. (B) Neu* TM domain sequence and those of five mutants, again designed to alter A*XXX*G and I*XXX*V motifs, and the CAT activities obtained for these sequences. CAT activities are means (after normalization to fusion protein concentration, and then to the value for GpA) of three or more independent measurements ± the standard error of the mean (SE). Western blots against maltose binding protein (MBP) are shown below the TOXCAT data to confirm expression levels of each fusion protein.

observed are still comparatively high when compared to the $G_{83}I$ negative control, suggesting that other residues in the TM domain can promote weak interactions between the Neu TM domains.

Similar analyses of the oncogenic Neu* TM domain produced quite different results. For this TM domain, single ($V_{663}L$ and $G_{665}L$) and double ($I_{659}A/V_{663}L$ and $A_{661}L/G_{665}L$) mutants of each motif were prepared, as well as a double mutant that targeted one residue in each motif ($V_{663}L/G_{665}L$). Comparison of the data shown in Figure 5B using a Student's *t* test (DOF = 4; $p = 0.05$) indicates that five of the six mutants produced no significant change in CAT activity, producing CAT activities statistically indistinguishable from that observed for the Neu* TM domain (data normalized to GpA, as shown in Figure 2). However, the double mutant $I_{659}A/V_{663}L$ significantly reduces CAT activity by ~70% [despite the fact that this sequence is predicted to have a more favorable ΔG_{app} of membrane insertion as calculated using the Hessa and von Heijne scale (*39*)], producing the most marked effect of all the mutations tested and indicating a substantial decrease in the level of self-association or rearrangement of the TM dimer. Furthermore, these results clearly show that the A*XXX*G motif is not crucial to the oligomerization of the oncogenic Neu* TM domain in a natural membrane bilayer, since mutation of these residues to leucine has no effect on self-association or conformation. On the contrary (and perhaps surprisingly), these results suggest that the I*XXX*V motif, previously suggested on the basis of evidence from FTIR data (*19*), stabilizes the mutant Neu* TM domain dimer and is almost exclusively favored over the A*XXX*G motif at the dimer interface in a natural membrane bilayer.

CONCLUSIONS

The Rat Neu TM Domain Self-Associates Strongly and the Effect of the Oncogenic Mutation Mirrors That Observed for the Human ErbB2 TM Domain. In this study, we have used the TOXCAT assay to measure helix−helix interactions of the wild-type and oncogenic rat Neu TM domains and have compared the results to similar measurements made in the past for the human ErbB2 TM domains (*38*). Similar to the human ErbB2 protein, the wild-type Neu TM domain forms strong oligomers in the absence of either ligand or the $V_{664}E$ mutation. These data further support the previously proposed theory that RTKs (receptor tyrosine kinases) can form oligomers in a manner independent of ligand binding, an occurrence that has been observed for several other RTKs (*33*, *53*). It is becoming more accepted that activation of these receptors may involve conformational changes in a preformed oligomer (e.g., dimer) rather than invoking oligomerization itself (*38*). The TOXCAT data for the oncogenic Neu $V_{664}E$ mutant (Neu*) we report here also mirror the results obtained for the human ErbB2 TM domain, suggesting that this position is crucial in both proteins. Insertion of this polar residue (E) did not result in any differences in secondary structure as indicated by CD, nor did it prevent membrane insertion (as shown by LD) and therefore most likely disrupts key helix−helix interactions, suggesting that the mutation may be involved in conformational changes in the TM domain dimer and supporting previous findings from computational mapping (*31*) and studies using synthetic peptides (*10*, *11*).

The Proto-Oncogenic Neu TM Dimer Has More Than One Stable Dimer Interface, while Dimerization of the Mutant Neu TM Strongly Favors a Single IXXXV Motif*. The results presented here show that residues I_{659} and V_{663} (I*XXX*V motif) stabilize the Neu* TM domain dimer, most probably by packing at the dimerization interface, and that the motif containing residues A_{661} and G_{665} has no effect on oligomerization. Although the A*XXX*G motif may seem to be a more likely candidate, because of the reduced packing constraints of the amino acids, neither single nor double mutants of this motif produce a noticeable reduction in the oligomerization propensity of the Neu* TM domain. Conversely, the wild-type Neu TM domain appears to adapt to mutation of either motif independently, with only a modest reduction in CAT activity

observed for either of the double mutants (similar to that seen for the $V_{664}E$ mutation in Neu*). Only upon elimination of both motifs does a more substantial decrease in the level of self-association occur. This is an interesting observation and raises the possibility that both the A*XXX*G and I*XXX*V motifs can support dimerization of the wild-type Neu TM domain, while the Neu* mutant selectively favors the I*XXX*V motif over the A*XXX*G motif in stabilization of helix−helix interactions. Our LD results also suggest that the conformations of the Neu and Neu* dimers may be different, as slight differences in their tilt angles were detected.

The importance of the $I_{659}XXXV_{663}$ motif in stabilizing the Neu* dimer has now been observed using FTIR measurements of synthetic TM peptides (*19*) and in this study using in vivo measurements in a natural membrane, strengthening the argument that this motif is favorable for interhelical association. The previously published model with I_{659} and V_{663} at the interface also contains residues L_{667}, I_{671}, V_{674}, and L_{679} in the interhelical region (*19*). This sequence of IVL is repetitive throughout the interface, indicating a like-for-like packing that may mimic a "knobs-into-holes" arrangement (*54*, *55*). This may implicate a motif similar to a tetrad motif, since previous experimental evidence suggests that Neu and its homologues form a right-handed coiled coil (*9*, *19*, *30*), which is dependent on specific arrangements of multiple residues (more than two) for effective oligomerization. Indeed, such a motif was suggested as a potential binding motif on the external surface of the wild-type human ErbB2 receptor in previous structural studies (*30*). This observation would explain the need for double mutations to cause a loss of the CAT signal in Neu*, as a single mutation ($V_{663}L$ or $G_{665}L$) may be easily offset by the strong interaction of other residues along the interface. The presence of a multiresidue tetrad motif would also explain the significant residual self-association observed in both Neu and Neu* upon mutation of one or both of the two-residue motifs, suggesting that other residues in the TM domain (such as the numerous Ile, Val, and Leu residues in the C-terminal portion of the TM) also play a role.

Oncogenic Mutation May Prevent Conformational Switching of TM Dimers. As mentioned above, our data indicate that both the A*XXX*G and I*XXX*V motifs support relatively high levels of dimerization for the wild-type Neu TM domain and appear to be equally favored at the dimer interface. This suggests that the wild-type Neu TM domain may easily adopt (at least) two conformations in the membrane, and these two types of dimers may correspond to active and inactive forms. In vivo, extracellular ligand binding may promote conformational switching from the inactive conformation by altering the structure sufficiently to result in the active conformer becoming the more energetically favorable. Such mechanisms are common in similar systems and have been reported for a number of RTKs (*33*, *53*, *56*).

Our data also indicate that the dimerization of the oncogenic Neu* mutant appears to strongly favor a single conformation stabilized by the I*XXX*V motif and is relatively unaffected by mutation of the A*XXX*G motif. One possible explanation for this behavior is that the $V_{664}E$ mutation in Neu* increases the energetic barrier between the active and inactive states, promoting the formation of one state (presumably the active state given the observed biological effect of the $V_{664}E$ mutation) and inhibiting formation of the other state (presumably the inactive state), thus preventing conformational switching back to the inactive state. Indeed, if one plots the two motifs on a model of

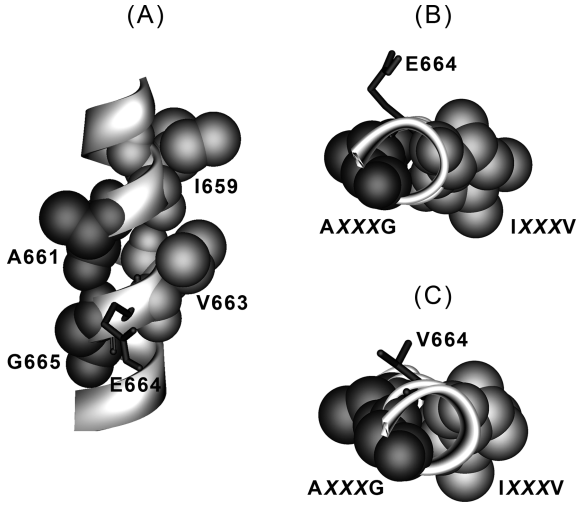

FIGURE 6: Conformational switching between interfaces may be impaired by the $V_{664}E$ mutation. (A) A molecular model of a single Neu* TM α-helix, illustrating the relative positions of the A*XXX*G and I*XXX*V motifs and E_{664}. Conformational switching from one interface to the other would involve rotation of each helix through approximately 180°. (B) The helical rotation in the Neu* TM domain may be impeded by the presence of the $V_{664}E$ mutation, which is much larger and more polar that the native Val found in wild-type Neu (C). The increased size of the glutamic acid residue and the presence of electrostatic forces may impede the switch from the $I_{659}XXXV_{663}$ to the $A_{661}XXXG_{665}$ interface.

the Neu* α-helix (Figure 6A, side view, and Figure 6B, top view), one can see that the E_{664} residue lies directly between them. One could easily imagine a situation in which rotation between the two conformations, one conformation stabilized by the I*XXX*V motif and the other by the A*XXX*G motif, would be extremely difficult if the polar glutamic acid residue was required to pass through the hydrophobic environment of the bilayer or near the Glu residue on the opposite helix, perhaps causing charge−charge repulsion. It is also possible that the previously proposed interaction of the glutamic acid with water molecules and polar lipid headgroups (*19*, *23*−*26*) may be unfavorably perturbed by any rotation of the helices. Another possibility is that the Glu mutation may cause a shift in the positioning of the TM domain dimer within the membrane, thus impeding rotation. Such a shift has been suggested by a recent study (*57*) which indicated that hydrophilic groups, when inserted at position 664, have a tendency to move closer to the membrane surface than more hydrophobic groups, presumably due to favorable interactions with the lipid headgroups and water molecules. In addition to polar interactions, the Glu residue in Neu* also has a larger side chain than the Val residue found in wild-type Neu (Figure 6C), introducing the possibility of increased steric hindrance to rotation of the helices. A final consideration is that the mutation causes a change in helical tilt (relative to the surface of the membrane bilayer). Changes in tilt angle have been previously observed by infrared spectroscopy (*18*) as well as the linear dichroism data reported here, where the higher degree of tilt observed in Neu* is consistent with the observation of a single helix−helix interaction site, while the lower degree of tilt in wt Neu would naturally accommodate multiple interaction sites. Continuing along this line of reasoning would also lead us to conclude that the active-state TM domain dimer contains an $I_{659}XXXV_{663}$ motif at the dimer interface, since this is the most critical interface found in oncogenic Neu*, but of course, this requires further study for confirmation.

This work provides novel experimental evidence in a natural membrane bilayer highlighting a striking difference in the behavior of the wild-type Neu TM domain and its oncogenic mutant, namely, the ability to adopt multiple conformations, as well as structural information that can be pursued in the future.

ACKNOWLEDGMENT

We thank Janet Crawford for peptide synthesis.

SUPPORTING INFORMATION AVAILABLE

NuPAGE gels of Neu and Neu* in SDS micelles and ATR-FTIR spectra of Neu and Neu* peptides in DMPC vesicles, including polarized spectra and deuterium exchange analysis. This material is available free of charge via the Internet at http://pubs.acs.org.

REFERENCES

1. Leahy, D. J. (2004) Structure and function of the epidermal growth factor (EGF/ErbB) family of receptors. *Adv. Protein Chem. 68*, 1–27.
2. Olayioye, M. A., Neve, R. M., Lane, H. A., and Hynes, N. E. (2000) The ErbB signalling network: Receptor heterodimerization in development and cancer. *EMBO J. 19*, 3159–3167.
3. Hynes, N. E., and Stern, D. F. (1994) The biology of Erb-B2/Neu/HER-2 and its role in cancer. *Biochim. Biophys. Acta 1198*, 165–184.
4. Bargmann, C. I., and Weinberg, R. A. (1988) Increased tyrosine kinase activity associated with the protein encoded by the activated Neu oncogene. *Proc. Natl. Acad. Sci. U.S.A. 85*, 5394–5398.
5. Bargmann, C. I., and Weinberg, R. A. (1988) Oncogenic activation of the Neu-encoded receptor protein by point mutation and deletion. *EMBO J. 7*, 2043–2052.
6. Weiner, D. B., Liu, J., Cohen, J. A., Williams, W. V., and Greene, M. I. (1989) A point mutation in the Neu oncogene mimics ligand induction of receptor aggregation. *Nature 339*, 230–231.
7. Bargmann, C. I., Hung, M.-C., and Weinberg, R. A. (1986) Multiple independent activations of the Neu oncogene by a point mutation altering the transmembrane domain of p185. *Cell 45*, 649–657.
8. Segatto, O., King, C. R., Pierce, J. H., Di Fiore, P. P., and Aaronson, S. A. (1988) Different structural alterations upregulate in vitro tyrosine kinase activity and transforming potency of the ErbB-2 gene. *Mol. Cell. Biol. 8*, 5570–5574.
9. Smith, S. O., Smith, C. S., Shekar, S., Peersen, O., Ziliox, M., and Aimoto, S. (2002) Transmembrane interactions in the activation of the Neu receptor tyrosine kinase. *Biochemistry 41*, 9321–9332.
10. Khemtemourian, L., Buchoux, S., Aussenac, F., and Dufourc, E. J. (2007) Dimerization of Neu/Erb2 transmembrane domain is controlled by membrane curvature. *Eur. Biophys. J. 36*, 107–112.
11. Khemtemourian, L., Lavielle, S., Bathany, K., Schnmitter, J. M., and Dufourc, E. J. (2006) Revisited and large-scale synthesis and purification of the mutated and wild type Neu/ErbB-2 membrane-spanning segment. *J. Pept. Sci. 12*, 361–368.
12. Houliston, R. S., Hodges, R. S., Sharom, F. J., and Davis, J. H. (2004) Characterisation of the proto-oncogenic and mutant forms of the transmembrane region of Neu in micelles. *J. Biol. Chem. 279*, 24073–24080.
13. Houliston, R. S., Hodges, R. S., Sharom, F. J., and Davis, J. H. (2003) Comparison of proto-oncogenic and mutant forms of the transmembrane region of the Neu receptor in TFE. *FEBS Lett. 535*, 39–43.
14. Brandt-Rauf, P. W., Rackovsky, S., and Pincus, M. R. (1990) Correlation of the structure of the transmembrane domain of the Neu oncogene-encoded p185 protein with its function. *Proc. Natl. Acad. Sci. U.S.A. 87*, 8660–8664.
15. Loudet, C., Khemtemourian, L., Aussenac, F., Gineste, S., Achard, M. F., and Dufourc, E. J. (2005) Bicelle membranes and their use for hydrophobic peptide studies by circular dichroism and solid state NMR. *Biochim. Biophys. Acta 1724*, 315–323.
16. Cao, H., Bangalore, L., Dompe, C., Bormann, B.-J., and Stern, D. F. (1992) An extra cysteine proximal to the transmembrane domain induces differential cross-linking of $p185^{neu}$ and $p185^{neu**}$. *J. Biol. Chem. 267*, 20489–20492.
17. Stanley, A. M., and Fleming, K. G. (2005) The transmembrane domains of ErbB receptors do not dimerize strongly in micelles. *J. Mol. Biol. 347*, 759–772.
18. Smith, S. O., Smith, C. S., and Bormann, B. J. (1996) Strong hydrogen bonding interactions involving a buried glutamic acid in the transmembrane sequence of the Neu/ErbB-2 receptor. *Nat. Struct. Biol. 3*, 252–258.
19. Beevers, A. J., and Kukol, A. (2006) The transmembrane domain of the mutant ErbB-2 receptor. A structure obtained from site-specific infrared dichroism and molecular dynamics simulations. *J. Mol. Biol. 361*, 945–953.
20. Sajot, N., and Genest, M. (2000) Structure prediction of the dimeric Neu/ErbB-2 transmembrane domain from multi-nanosecond molecular dynamics simulations. *Eur. Biophys. J. 28*, 648–662.
21. Aller, P., Voiry, L., Garnier, N., and Genest, M. (2005) Molecular dynamics (MD) investigations of preformed structures of the transmembrane domain of the oncogenic Neu receptor in a DMPC bilayer. *Biopolymers 77*, 184–197.
22. Sternberg, M. J. E., and Gullick, W. J. (1989) Neu receptor dimerization. *Nature 339*, 587.
23. Garnier, N., Crouzy, S., and Genest, M. (2003) Molecular dynamics simulations of the transmembrane domain of the oncogenic ErbB-2 receptor dimer in a DMPC bilayer. *J. Biomol. Struct. Dyn. 21*, 179–199.
24. van der Ende, B. M., Sharom, F. J., and Davis, J. H. (2004) The transmembrane domain of Neu in a lipid bilayer: Molecular dynamics simulations. *Eur. Biophys. J. 33*, 596–610.
25. Beevers, A. J., and Kukol, A. (2006) Systematic molecular dynamics searching in a lipid bilayer: Application to the Glycophorin A and oncogenic ErbB-2 transmembrane domains. *J. Mol. Graphics Modell. 25*, 226–233.
26. Soumana, O. S., Aller, P., Garnier, N., and Genest, M. (2005) Transmembrane peptides from tyrosine kinase receptor. Mutation-related behaviour in a lipid bilayer investigated by molecular dynamics simulations. *J. Biomol. Struct. Dyn. 23*, 91–99.
27. Sternberg, M. J. E., and Gullick, W. J. (1990) A sequence motif in the transmembrane region of growth factor receptors with tyrosine kinase activity mediates dimerization. *Protein Eng. 3*, 245–248.
28. Russ, W. P., and Engelman, D. M. (2000) The GXXXG motif: A framework for transmembrane helix-helix association. *J. Mol. Biol. 296*, 911–919.
29. Cao, H., Bangalore, L., Bormann, B. J., and Stern, D. F. (1992) A subdomain in the transmembrane domain is necessary for p185 Neu* activation. *EMBO J. 11*, 923–932.
30. Bocharov, E. V., Mineev, K. S., Volynsky, P. E., Ermolyuk, Y. S., Tkach, E. N., Sobol, A. G., Chupin, V. V., Kirpichnikov, M. P., Efremov, R. G., and Arseniev, A. S. (2008) Spatial structure of the dimeric transmembrane domain of the growth factor receptor ErbB-2 presumably corresponding to the receptor active site. *J. Biol. Chem. 283*, 6950–6956.
31. Fleishman, S. J., Schlessinger, J., and Ben-Tal, N. (2002) A putative molecular-activation switch in the transmembrane domain of ErbB-2. *Proc. Natl. Acad. Sci. U.S.A. 99*, 15937–15940.
32. Escher, C., Cymer, F., and Schneider, D. (2009) Two GXXXG-like motifs facilitate promiscuous interactions of the human ErbB transmembrane domains. *J. Mol. Biol. 389*, 10–16.
33. Yu, X., Sharma, K. D., Takahashi, T., Iwamoto, R., and Mekada, E. (2002) Ligand-independent dimer formation of epidermal growth factor receptor (EGFR) is a step separable from ligand-induced EGFR signaling. *Mol. Biol. Cell 13*, 2547–2557.
34. Moriki, T., Maruyama, H., and Maruyama, I. N. (2001) Activation of performed EGF receptor dimers by ligand-induced rotation of the transmembrane domain. *J. Mol. Biol. 311*, 1011–1026.
35. Russ, W. P., and Engelman, D. M. (1999) TOXCAT: A measure of transmembrane helix association in a biological membrane. *Proc. Natl. Acad. Sci. U.S.A. 96*, 863–868.
36. Manavalan, P., and Johnson, W. C. (1987) Variable selection method improves the prediction of protein secondary structure from circular dichroism spectra. *Anal. Biochem. 167*, 76–85.
37. Sreerama, N., Venyaminov, S. Y., and Woody, R. W. (2000) Estimation of protein secondary structure from circular dichroism spectra: Inclusion of denatured proteins with native proteins in the analysis. *Anal. Biochem. 287*, 243–251.
38. Mendrola, J. M., Berger, M. B., King, M. C., and Lemmon, M. A. (2002) The single transmembrane domains of ErbB receptors self-associate in cell membranes. *J. Biol. Chem. 277*, 4704–4712.
39. Hessa, T., Meindl-Beinker, N., Bernsel, A., Kim, J., Sato, Y., Lerch, M., Lundin, C., Nilsson, I., White, S. H., and Von Heijne, G. (2007) Molecular code for transmembrane-helix recognition by the sec61 translocon. *Nature 450*, 1026–1030.
40. MacKenzie, K. R., Prestegard, J. H., and Engelman, D. M. (1997) A transmembrane helix dimer: Structure and implications. *Science 276*, 131–133.
41. Lemmon, M. A., Flanagan, J. M., Hunt, J. F., Adair, B. D., Bormann, B.-J., Dempsey, C. E., and Engelman, D. M. (1992) Glycophorin A

dimerization is driven by specific interactions between transmembrane α-helices. *J. Biol. Chem. 267*, 7683–7689.
42. Freeman-Cook, L. L., Dixon, A. M., Frank, J. B., Xia, Y., Ely, L., Gerstein, M., Engelman, D. M., and DiMaio, D. (2004) Selection and characterization of small random transmembrane proteins that bind and activate the platelet-derived growth factor beta receptor. *J. Mol. Biol. 338*, 907–920.
43. Dixon, A. M., Stanley, B. J., Matthews, E. E., Dawson, J. P., and Engelman, D. M. (2006) Invariant chain transmembrane domain trimerization: A step in MHC class II assembly. *Biochemistry 45*, 5228–5234.
44. Li, R., Gorelik, R., Nanda, V., Law, P. B., Lear, J. D., DeGrado, W. F., and Bennett, J. S. (2004) Dimerization of the transmembrane domain of the integrin α_{iib} subunit in cell membranes. *J. Biol. Chem. 279*, 26666–26673.
45. Rath, A., Gilibowicka, M., Nadeau, V. G., Chen, G., and Deber, C. M. (2009) Detergent binding explains anomalous SDS-PAGE migration of membrane proteins. *Proc. Natl. Acad. Sci. U.S.A. 106*, 1760–1765.
46. Rodger, A., Rajendra, J., Marrington, R., Ardhammar, M., Norden, B., Hirst, J. D., Gilbert, T. B., Dafforn, T. R., Halsall, D. J., Woolhead, C. A., Robinson, C., Pinheiro, T. J. T., Kazlauskaite, J., Seymour, M., Perez, N., and Hannon, M. J. (2002) Flow oriented linear dichroism to probe protein orientation in membrane environments. *Phys. Chem. Chem. Phys. 4*, 4051–4057.
47. Marrington, R., Dafforn, T. R., Halsall, D. J., and Rodger, A. (2004) Micro-volume couette flow sample orientation for absorbance and fluoresence linear dichroism. *Biophys. J. 87*, 2002–2012.
48. Conner, M., Hicks, M. R., Dafforn, T. R., Knowles, T. J., Ludwig, C., Staddon, M., Overduin, U. L., Gunther, J., Thome, M., Wheatley, D. R., Poyner, D. R., and Conner, A. C. (2008) Functional and biophysical analysis of the C-terminus of the CGRP-receptor: A family B GPCR. *Biochemistry 47*, 8434–8444.
49. Hicks, M. R., Damianoglou, A., Rodger, A., and Dafforn, T. R. (2008) Folding and membrane insertion of the pore-forming peptide gramicidin occur as a conserted process. *J. Mol. Biol. 383*, 358–366.
50. Oates, J., Hicks, M., Dafforn, T. R., DiMaio, D., and Dixon, A. M. (2008) In vitro dimerization of the bovine papillomavirus E5 protein transmembrane domain. *Biochemistry 47*, 8985–8992.
51. Ardhammar, M., Mikati, M., and Norden, B. (1998) Chromophore orientation in liposome membranes probed with flow linear dichroism. *J. Am. Chem. Soc. 120*, 9957–9958.
52. Gullick, W. J., Bottomley, A. C., Lofts, F. J., Doak, D. G., Mulvey, D., Newman, R., Crumpton, M. J., Sternberg, M. J. E., and Campbell, I. D. (1992) Three dimensional structure of the transmembrane region of the proto-oncogenic and oncogenic forms of the Neu protein. *EMBO J. 11*, 43–48.
53. Seubert, N., Royer, Y., Staerk, J., Kubatzky, K. F., Moucadel, V., Krishnakumar, S., Smith, S. O., and Constantinescu, S. N. (2003) Active and inactive orientations of the transmembrane and cytosolic domains of the Erythropoietin receptor dimer. *Mol. Cell 12*, 1239–1250.
54. Crick, F. H. C. (1953) The packing of α-helices: Simple coiled-coils. *Acta Crystallogr. 6*, 689.
55. Harrington, S. E., and Ben-Tal, N. (2009) Structural determinants of transmembrane helical proteins. *Structure 17*, 1092–1103.
56. Schlessinger, J. (2000) Cell signalling by receptor tyrosine kinases. *Cell 103*, 211–225.
57. Shahidullah, K., Krishnakumar, S. S., and London, E. (2010) The effect of hydrophillic substitutions and anionic lipids upon the transverse positioning of the transmembrane helix of the ErbB2 (Neu) protein incorporated into model membrane vesicles. *J. Mol. Biol. 396*, 209–220.